The Connection between Carnot and CAPE Formulations of TC Potential Intensity

RAPHAËL ROUSSEAU-RIZZI,[a] TIMOTHY M. MERLIS,[b] AND NADIR JEEVANJEE[c]

[a] *Lorenz Center, Department of Earth and Planetary Sciences, Massachusetts Institute of Technology, Cambridge, Massachusetts*
[b] *Department of Atmospheric and Oceanic Sciences, McGill University, Montreal, Quebec, Canada*
[c] *NOAA/Geophysical Fluid Dynamics Laboratory, Princeton, New Jersey*

(Manuscript received 6 May 2021, in final form 5 October 2021)

ABSTRACT: Tropical cyclone (TC) potential intensity (PI) theory has a well-known form, consistent with a Carnot cycle interpretation of TC energetics, which relates PI to mean environmental conditions: the difference between surface and TC outflow temperatures and the air–sea enthalpy disequilibrium. PI has also been defined as a difference in convective available potential energy (CAPE) between two parcels, and quantitative assessments of future changes make use of a numerical algorithm based on this definition. Here, an analysis shows the conditions under which these Carnot and CAPE-based PI definitions are equivalent. There are multiple conditions, not previously enumerated, which in particular reveal a role for irreversible entropy production from surface evaporation. This mathematical analysis is verified by numerical calculations of PI's sensitivity to large changes in surface-air relative humidity. To gain physical insight into the connection between the CAPE and Carnot formulations of PI, we use a recently developed analytic theory for CAPE to derive, starting from the CAPE-based definition, a new approximate formula for PI that nearly recovers the previous Carnot PI formula. The derivation shows that the difference in undilute buoyancies of saturated and environmental parcels that determines CAPE PI can in fact be expressed as a difference in the parcels' surface moist static energy, providing a physical link between the Carnot and CAPE formulations of PI. This combination of analysis and physical interpretation builds confidence in previous numerical CAPE-based PI calculations that use climate model projections of the future tropical environment.

KEYWORDS: Convection; Tropical cyclones; Climate change

1. Introduction

Tropical cyclone (TC) or hurricane potential intensity (PI) theory is the maximum TC intensity that an environment can sustain (Emanuel 1986, 2003). PI is expressed either as a minimum surface pressure or maximum surface wind speed that is determined from the thermodynamic environment. Though most TCs do not reach their PI (≈75 m s^{-1} wind speed in Earth's tropics), PI has been widely used to interpret the climatology, climate variability, and future climate changes of TC activity (e.g., Emanuel et al. 2004; Camargo et al. 2007; Emanuel et al. 2008; Knutson et al. 2010; Sobel et al. 2016).

There have been critiques of PI theory based on its assumptions of axisymmetric TC structure and boundary layer thermodynamics (e.g., Persing and Montgomery 2003; Smith et al. 2008). In spite of these known limitations, PI is central to a ventilation index that is a useful predictor of intensification in individual tropical cyclones (Tang and Emanuel 2012). Furthermore, PI accounts for the simulated TC intensity increase in TC forecast simulations with warmed temperatures from climate change projections (Knutson and Tuleya 2004) and the sensitivity of TC intensity in single-storm convection-permitting simulations to temperature changes (Nolan et al. 2007; Wang et al. 2014; Ramsay et al. 2020). There are also climate-relevant idealized TC simulations (Merlis and Held 2019) with multiple TCs where PI accounts for changes in the TC intensity of the most intense TCs under varied sea surface temperature (Zhou et al. 2014; Merlis et al. 2016). Given these results, it is fair to consider PI a useful perturbation or scaling theory for intensity changes of the most intense TCs. It is PI's temperature sensitivity—where PI has proven useful—that motivates this research, rather than the detailed dynamics of individual TCs—where PI has limitations.

PI has been assessed in future climate warming scenarios by Emanuel (1987) and subsequent generations of climate model simulations have been thoroughly examined (Vecchi and Soden 2007; Sobel and Camargo 2011; Emanuel 2013; Sobel et al. 2016). The tropical-mean PI (assessed over tropical oceans) typically increases in proportion to the tropical surface warming at a rate of ≈1 m s^{-1} K^{-1}. This increase in PI, from a climatological value of ≈75 m s^{-1}, corresponds to fractional sensitivity of about 1.5% K^{-1}. Superimposed on this tropical-mean increase in PI are geographic variations that are substantial in magnitude (~5× larger than the tropical-mean change with some regional decreases) and uncertain as a result of their dependence on regional climate projections (Vecchi and Soden 2007; Rousseau-Rizzi and Emanuel 2021).

PI theory has a physical interpretation in terms of a Carnot cycle and a corresponding approximate formula (described below) that accounts for the tropical-mean PI increase under global warming (Emanuel 1987, 2003; Sobel et al. 2016). However, published assessments of observed PI trends or future climate projections of PI in the recent generations of Coupled Model Intercomparison Project (CMIP) simulations have exclusively made use of a definition of PI that is a difference in convective available potential energy (CAPE), which is implemented as an iterative, numerical algorithm for PI (Bister and Emanuel 2002). Bister and Emanuel (2002) described the algorithm, and a numerical implementation of it has been publicly

Corresponding author: Timothy M. Merlis, timothy.merlis@mcgill.ca

DOI: 10.1175/JCLI-D-21-0360.1

disseminated by K. Emanuel (ftp://texmex.mit.edu/pub/emanuel/TCMAX/). Given the importance of PI in scientific and public discourse about climate change's effects on TC intensity, there is a need for a better understanding of the relationship between the quantitative analyses that use the publicly disseminated PI-CAPE code and the Carnot PI formula, which offers a physical understanding of the origin of the tropical-mean increase in PI under warming. Here, we present an analysis of the assumptions under which the CAPE-based and Carnot PI expressions are equivalent and derive a new approximate PI formula from the CAPE-based PI that is evaluated analytically using the Romps (2016) theory for CAPE.

Our analysis of the equivalence of the existing PI forms considers the standard thermodynamic cycle associated with PI theories (e.g., Emanuel 1988a, Fig. C1), where the mechanical work done is equal to a CAPE difference. We allow for phase disequilibrium in moist thermodynamics, consistent with the standard physical picture of increasing relative humidity along the surface inflow branch of the TC, and find that there is an irreversible entropy production term in the TC cycle that has previously been ignored. This term needs to be included to reconcile PI forms. Further, we find that unless an additional correction term is introduced to account for heat capacity changes in reversible thermodynamics formulations, the Carnot PI will overestimate the amount of work the system can produce and will substantially exceed the CAPE-defined PI. To quantitatively assess the success of these newly described correction terms, we numerically compute PI over a wide range of environmental surface relative humidities and find that they succeed in bridging the differences in the existing forms of PI.

To shed light on the physical picture underlying the connection between the CAPE definition of PI and the Carnot form, we also derive a new, approximate form of PI starting from the CAPE definition. This derivation builds on recent progress in understanding moist convection in the tropical atmosphere by viewing deep convection as an entraining plume that is neutrally buoyant with respect to the environment (Singh and O'Gorman 2013). This line of research has explained the increase in CAPE with warming (Singh and O'Gorman 2013; Seeley and Romps 2015), which is simulated by both cloud-system-resolving models and general circulation models (Singh and O'Gorman 2013; Sobel and Camargo 2011). It has also formed the basis of new theories for the relative humidity and thermal stratification of the tropical atmosphere (Romps 2014, 2016). In particular, Romps (2016) gives an approximate form of CAPE that can be evaluated analytically. In what follows, this CAPE theory is used to derive an approximate PI formula. For Earthlike conditions, the newly derived CAPE-based PI formula is nearly identical to the well-known Carnot PI formula.

We review PI in section 2, assess the conditions under which the CAPE and Carnot PI formulations are equivalent in section 3, present physical intuition for how the CAPE PI and Carnot formula are connected and the results of a systematic derivation of a CAPE-based approximate PI formula in section 4, compare the CAPE-based PI to the results of numerical CAPE–PI algorithm in section 5, and conclude in section 6.

2. Potential intensity

a. Carnot cycle form

The PI theory developed by Emanuel (1986) assumes axisymmetric structure, angular momentum conserving flow and thermal wind balance away from the boundary layer, and a well-mixed boundary layer. Here only velocity PI, denoted PI, is considered, though results can be translated to pressure PI with a suitable TC structure model (e.g., Chavas et al. 2017).

The approximate formula that has the Carnot engine interpretation considers an isothermal enthalpy increase $\propto k_s^* - k_a$ at the warm sea surface temperature T_s, isentropic expansion in the ascent of the TC eyewall, isothermal enthalpy loss at the cold outflow temperature T_o near the tropopause, and isentropic compression to the surface. This results in the following equation (Emanuel 2003):

$$\mathrm{PI}_k^2 \approx \frac{c_k}{c_d}\frac{T_s - T_o}{T_o}\left(k_s^* - k_a\right), \tag{1}$$

with surface (skin) temperature T_s, TC outflow temperature T_o, drag coefficient for enthalpy c_k, and drag coefficient for momentum c_d. Here, moist enthalpy is defined $k = c_pT + Lr$, where c_p is the heat capacity at constant pressure of dry air, L is the latent heat of vaporization, r is the water vapor mixing ratio, and the contribution of water species to heat capacity has been neglected. The moist enthalpy difference is between the saturated, indicated by *, sea surface $k_s^* = c_pT_s + Lr^*(T_s)$ and the surface air $k_a = c_pT_a + Lr_a$. The subscript k indicates that this is an enthalpy-defined PI. The factor $(T_s - T_o)/T_o$ is often described as a thermodynamic efficiency, and the temperature in the denominator depends on whether dissipative heating is recycled (Bister and Emanuel 1998), which gives rise to the T_o in the denominator, or not (Emanuel 1986), in which case T_s is in the denominator and it is a genuine Carnot efficiency. In reality, if dissipative heating is recycled, the TC becomes a "zero work engine" and strictly speaking, this factor is not representative of a thermodynamic efficiency anymore. Here PI bounds the maximum magnitude of the surface winds. We note that exact derivations of (1) were provided by Bister and Emanuel (1998) and Rousseau-Rizzi and Emanuel (2019), albeit with a different interpretation that does not require the full secondary circulation to correspond to a Carnot cycle.

Carnot PI is also commonly written as a function of the entropy s difference, indicated by the subscript PI_s, between the near surface and the sea surface (e.g., Bryan and Rotunno 2009):

$$\mathrm{PI}_s^2 \equiv \frac{c_k}{c_D}\left(\frac{T_s}{T_o}\right)\left(s_s^* - s_b\right)(T_s - T_o). \tag{2}$$

This differs only modestly from (1) for Earthlike ≈1 K air–sea temperature differences.

To estimate the climatological PI, the air–sea enthalpy disequilibrium can be approximated as follows:

$$\mathrm{PI}_k^2 \approx \frac{c_k}{c_d}\frac{T_s - T_o}{T_o}Lr^*(T_s)(1 - \mathcal{H}_b),$$

with near-surface boundary layer relative humidity $\mathcal{H}_b$ and where the air–sea temperature difference is assumed to be small. This is an adequate first approximation for Earth's tropics, though neglecting the air–sea temperature difference is not quantitatively accurate for near-saturation conditions. Using representative values of $T_s = 300$ K, $T_o = 200$ K, equal drag coefficients $c_k/c_d = 1$, $L = 2.5 \times 10^6$ J kg^{-1}, $r^*(T_s) = 2.3 \times 10^{-2}$, and $\mathcal{H}_b = 0.8$, the velocity PI is ≈76 m s^{-1}. This is similar to the values found using the CAPE-based PI algorithm (section 5b) for Earth's tropics in reanalyses and radiosonde soundings (Bister and Emanuel 2002; Emanuel et al. 2013; Wing et al. 2015; Sobel et al. 2016). Relative humidity only enters this form of the Carnot PI directly through the thermodynamic disequilibrium term. The first PI derivation introduced by Emanuel (1986), which assumes gradient wind balance above the boundary layer, provides a bound on the azimuthal wind at the top of the boundary layer. In that formulation, T_s in the numerator of the thermodynamic efficiency becomes T_{LCL}, the temperature at the lifting condensation level (LCL). This introduces an additional dependence on boundary layer relative humidity, but the formula is otherwise identical.

Though there has been substantial discussion of upper troposphere and lower stratosphere temperature changes—affecting T_o—on PI (Emanuel et al. 2013; Vecchi et al. 2013; Gilford et al. 2017), these changes do not dominate the observed trends in recent decades (Wing et al. 2015). Rather, the air–sea disequilibrium increase with warming largely accounts for the tropical-mean PI increase.

b. CAPE-based PI algorithm

PI is related to CAPE through the line integral around the TC cycle (Emanuel 1988b; Bister and Emanuel 2002). The velocity PI is given by the following difference between CAPE, denoted with subscript C, of the following two parcels:

$$\mathrm{PI}_C^2 = \frac{T_s}{T_o}\frac{c_k}{c_d}(\mathrm{CAPE}^* - \mathrm{CAPE}^m), \tag{3}$$

with the CAPE of a saturated parcel lifted from T_s at TC eyewall pressure denoted CAPE* (saturation CAPE) and a parcel with environmental relative humidity, surface air temperature, and TC eyewall pressure denoted CAPE^m (radius of maximum winds CAPE). In the next section, we present the conditions under which the CAPE–PI formula (3) is equivalent to the Carnot expression (1).

The algorithm of Bister and Emanuel (2002), which makes use of this PI form, iterates to adjust the parcel pressure used in these two CAPE calculations to that of the TC eyewall, taken to be the pressure PI. Because this pressure change relative to the environment is common to the two CAPEs used to determine the velocity PI, it has a modest ≲10% effect on PI_C, consistent with the PI pressure being ≈10% lower than the environmental surface pressure in Earth's tropics. In contrast, including the pressure change in saturation CAPE only, consistent with the slightly different model of Emanuel (1988a) can provoke an unstable "hypercane" transition at very high surface temperatures. We will neglect this pressure dependence in our derivations (sections 3 and 4) and numerically assess it in section 5.

This CAPE algorithm has been used for all quantitative analyses of PI changes in CMIP simulations of climate change (e.g., Vecchi and Soden 2007; Sobel et al. 2019). Yet, it is not straightforward to identify why (3) increases as the climate warms, in contrast to (1), which has increases that typically scale with evaporation increases. One of the contributions of this research is to develop this understanding. For example, one might ask if the numerically evaluated (3) increase is related to the tropical environment's projected increase in CAPE (e.g., Sobel and Camargo 2011). Our derivation shows that PI changes determined via the CAPE formula are *not*, in fact, related to environmental stratification changes (see also Garner 2015 for discussion of the limited role of environmental CAPE in a given climate).

3. When are Carnot and CAPE-based PI equal?

To establish the conditions required for the equivalence between PI forms, we define a PI thermodynamic cycle that has two isothermal and two isentropic legs, illustrated in Fig. 1. The isothermal surface inflow (i) leg is assumed to occur at constant total pressure, which does not account for the surface pressure gradient within a mature storm. Entropy is constant along the ascent (a) leg, which is assumed to be saturated throughout. The outflow (o) leg is assumed to match an isothermal and saturated environment, but pressure is not constant. The descent (d) leg is isentropic, but not saturated throughout, and in the unsaturated part of the descent, the water vapor mixing ratio is constant. For reversible thermodynamics, the total water mixing ratio is constant along both the ascent and the descent legs and varies along the isothermal inflow and outflow legs. We note that this cycle is designed to satisfy the assumptions of various PI forms and, in its integrated form, to establish a comparison between these forms, but as discussed previously (Emanuel 1988b; Rousseau-Rizzi and Emanuel 2019; Rousseau-Rizzi et al. 2021), it need not represent the actual cycle an air parcel undergoes along the TC secondary circulation. Hence the labels of the cycle legs are meant to give a sense of the direction of integration of the thermodynamic cycle, more so than to establish a direct comparison to the secondary circulation. We make no claim, for example, that the air in TCs is actually saturated at the surface before ascending in the eyewall, even though this occurs in the thermodynamic cycle presented here. In this context, taking pressure to be constant at the surface is an approximation to the PI model of Emanuel (1988b), which accounts for the environmental surface conditions, but not to the PI model of Bister and Emanuel (1998), which depends on local conditions in the eyewall.

In this section, we first review the basis of the CAPE PI definition by showing that the difference in CAPE is equal to the mechanical work produced by this thermodynamic cycle. Then, we integrate suitable thermodynamic equations for TCs—allowing for evaporation in the subsaturated air—for reversible and pseudoadiabatic cases over the cycle. Here, we cannot use the simplified differential forms of moist thermodynamic equations that assume phase equilibrium [e.g., reversible thermodynamics, Emanuel (1994) or those of Bryan and Rotunno (2009) for pseudoadiabatic thermodynamics] because a PI sufficiently large to sustain a real TC requires evaporation of liquid water into

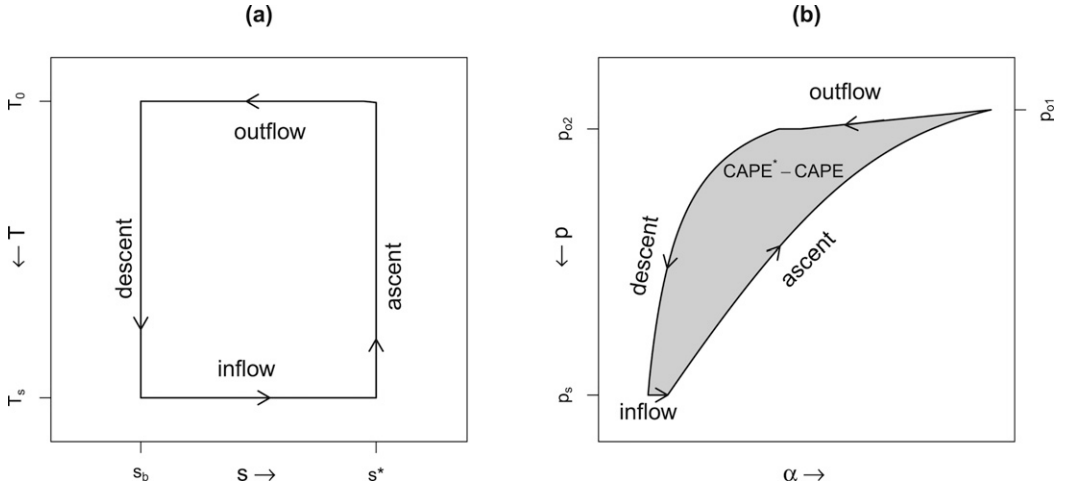

FIG. 1. (a) Tropical cyclone thermodynamic cycle in temperature–entropy coordinates with saturation sea surface entropy s^*, boundary layer entropy s_b, surface temperature T_s, and outflow temperature T_o. (b) Tropical cyclone thermodynamic cycle in specific volume–pressure coordinates with surface pressure p_s, outflow pressures p_{o1} and p_{o2}, with the shaded area equal to $\text{CAPE}^* - \text{CAPE}^m$.

unsaturated air. (Substantial values of PI could, in theory, exist for dry or fully saturated reversible moist thermodynamics, though this requires large ≈10-K air–sea temperature differences, which is unlike conditions observed over tropical oceans.) The results of these integrals relate existing PI forms and allows us to present "correction" terms that provide a precise connection between the existing PI equations.

a. CAPE and the work of the TC thermodynamic cycle

Here we show the equivalence between the mechanical work produced by the thermodynamic cycle, given by the cycle integral of αdp, and the CAPE difference (Emanuel 1994). We start by splitting the cycle integral into the different legs:

$$\oint \alpha\, dp = \int_i \alpha\, dp + \int_a \alpha\, dp + \int_o \alpha\, dp + \int_d \alpha\, dp,$$

with subscripts i, a, o, and d denoting inflow, ascent, outflow, and descent legs, respectively. We note again that these labels denote a direction of integration, and not necessarily a secondary circulation.

Since we assume surface pressure is constant (we do not iterate on surface pressure), the "i" leg integrates to 0 and we have

$$\oint \alpha\, dp = \int_{p_{o1}}^{p_s} \alpha_a\, dp + \int_{p_{o2}}^{p_{o1}} \alpha_o\, dp + \int_{p_s}^{p_{o2}} \alpha_d\, dp,$$

where p_s, p_{o1}, and p_{o2} are surface pressure and the lowest and highest outflow pressures (Fig. 1). The α_a is along the ascent leg, α_d is along the descent leg, and α_o is along the isothermal outflow leg. Equivalently, we can write

$$\oint \alpha\, dp = \int_{p_{o1}}^{p_s} \alpha_a dp - \int_{p_{o1}}^{p_{o2}} \alpha_o\, dp - \int_{p_{o2}}^{p_s} \alpha_e\, dp + \int_{p_{o2}}^{p_s} \alpha_e dp - \int_{p_{o2}}^{p_s} \alpha_d dp,$$

where α_e is the environmental α. Finally, if the environmental profile matches the outflow leg, we can see that

$$\oint \alpha dp = \int_{p_{o1}}^{p_s} (\alpha_a - \alpha_e) dp - \int_{p_{o2}}^{p_s} (\alpha_d - \alpha_e) dp + \int_{p_{o1}}^{p_{o2}} (\alpha_e - \alpha_o) dp$$

$$= \text{CAPE}^* - \text{CAPE}^m + 0.$$

This equivalence of the TC cycle work and CAPE difference is the basis of the CAPE–PI definition that is used in the numerical algorithm (Bister and Emanuel 2002). It is, however, important to note that we assumed the surface pressure is constant to arrive at this result, while a commonly discussed reason for introducing the *iterative* CAPE-based PI algorithm is that it accounts for the enhancement in surface enthalpy fluxes due to the pressure drop near the center of a mature cyclone, which further strengthens the storm. We also note that this equivalence requires the outflow profile of the TC, usually taken at the radius of zero tangential wind, to match the environmental profile.

b. Work integrals around the PI thermodynamic cycle

1) INTEGRATION FOR REVERSIBLE THERMODYNAMICS

We begin with the reversible moist entropy form of Emanuel (1994) given by

$$s = (c_p + r_t c_l)\ln T - R\, \ln p_d + \frac{Lr}{T} - r R_v\, \ln(\mathcal{H}),$$

with total water r_t and specific heat of liquid c_l, and the corresponding moist enthalpy is $k = (c_p + r_t c_l)T + Lr$. We then combine the differential of both variables along with the ideal gas law, Kirchhoff's relation, and the equation of Clausius–Clapeyron, to yield

$$Tds = dk - \alpha_d dp + c_l T(\ln\, T - 1) dr_t - T R_v \ln(\mathcal{H}) dr, \qquad (4)$$

where changes in total water content are allowed and the last term accounts for irreversible entropy production, which is always positive. We recall that p denotes total air pressure, and even though α_d denotes dry air specific volume, this formula does not neglect virtual effects.

To verify the equivalence of the three PI formulations, we need to integrate (4) in two different ways. First, we integrate (4) along the isothermal, constant pressure, inflow leg only, which yields

$$\left(s_s^* - s_b\right)T_s = \left(k_s^* - k_b\right) + c_l T_s(\ln\ T_s - 1)\left(r_s^* - r_b\right) + T_s \Delta s_{\text{irr}}, \tag{5}$$

where

$$\Delta s_{\text{irr}} = R_v\left[r_b \ln(\mathcal{H}_b) + \varepsilon\ln\left(\frac{r_s^* \mathcal{H}_b}{r_b}\right)\right]$$

is the total irreversible entropy production associated with evaporating water into unsaturated air at an initial boundary layer relative humidity $\mathcal{H}_b$ and at constant temperature and total pressure, until saturation (see appendix A) and ε is the ratio of dry air and vapor gas constants. The second term on the right-hand side (RHS) of (5) arises because of changes in heat capacity due to changes in total water mixing ratio. The second integral we need to perform is around the full thermodynamic cycle, and we will express it as

$$\oint \alpha_d dp = \oint dk + \oint s\, dT + \oint c_l T(1 - \ln\ T) dr_t - \oint T R_v \ln(\mathcal{H}) dr.$$

If we neglect the effects of water vapor on specific volume, the left-hand side of the equation (LHS) is equal to the mechanical work produced by the cycle, which we have shown to be equal to the difference between sea surface saturation CAPE and boundary layer CAPE. By definition, the integral of the first term on the RHS vanishes when integrated over the full cycle. Interestingly, the integral of the last term on the RHS is zero along the ascent, outflow, and descent legs, so that the integral along the full cycle is equal to the integral along the inflow leg only (see appendix A). In other words, in this cycle, irreversible entropy production due to evaporation into unsaturated air only happens near the sea surface. Finally, we get

$$\begin{aligned}(\text{CAPE}^* - \text{CAPE}^m) = \left(s_s^* - s_b\right)(T_s - T_o) + c_l\big[T_s(1 - \ln\ T_s) \\ - T_o(1 - \ln\ T_o)\big]\left(r_s^* - r_b\right) - T_s \Delta s_{\text{irr}}.\end{aligned} \tag{6}$$

Or, combining (5) and (6), we can express the reference CAPE difference as a function of the near-surface enthalpy difference, which yields

$$\begin{aligned}(\text{CAPE}^* - \text{CAPE}^m) = \left(\frac{T_s - T_o}{T_s}\right)\left(k_s^* - k_b\right) + c_l T_o \ln\left(\frac{T_o}{T_s}\right) \\ \times\left(r_s^* - r_b\right) - T_o \Delta s_{\text{irr}}.\end{aligned} \tag{7}$$

The irreversible entropy production term is negligible for Earthlike tropical conditions ($\mathcal{H}_b = 0.8$), but not for smaller $\mathcal{H}_b$. The second terms on the RHS of both (6) and (7), which are associated with changes in heat capacity, are not small. In (6), the heat capacity correction is of the same magnitude as the main term $\left(s_s^* - s_b\right)(T_s - T_o)$. On its own, neglecting this term while maintaining variable heat capacity in the definition of s would lead to order 1 discrepancies between PI forms. However, changes in heat capacity (and L) are often neglected in enthalpy and entropy definitions for PI computations, which cancels most of this term. These heat-capacity-related terms vanish for certain definitions of pseudoadiabatic thermodynamic variables, to which we turn next.

2) Integration for pseudoadiabatic thermodynamics

We start with the approximation of Bryan (2008), which neglects the contribution of water vapor to heat capacity, assumes constant $L = L_0$, and adjusts the value of this constant to minimize errors. The corresponding definitions of entropy and enthalpy are

$$\hat{s} = c_p \ln\ T - R_d \ln\ p_d + \frac{L_0 r}{T} - r R_v\ \ln(\mathcal{H}),$$

and $\hat{k} = c_p T + L_0 r$, where $\widehat{(\cdot)}$ denotes pseudoadiabatic thermodynamics of Bryan (2008). From there, similarly to the process for reversible thermodynamics, we get the equation

$$T d\hat{s} = d\hat{k} - \alpha_d dp - T R_v \ln(\mathcal{H}) dr,$$

which we can integrate to get a similar result to the reversible thermodynamics case. In contrast to the reversible case, there is no term accounting for changes in heat capacity, which is a constant. We once again neglect the effects of water vapor on specific volume to establish an equivalence with the CAPE difference. We get

$$\left(\widehat{\text{CAPE}}^* - \widehat{\text{CAPE}}^m\right) = \left(\hat{s}_s^* - \hat{s}_b\right)(T_s - T_o) - T_s \Delta s_{\text{irr}}, \tag{8}$$

which can also be expressed as an enthalpy difference

$$\left(\widehat{\text{CAPE}}^* - \widehat{\text{CAPE}}^m\right) = \left(\frac{T_s - T_o}{T_s}\right)\left(\hat{k}_s^* - \hat{k}_b\right) - T_o \Delta s_{\text{irr}}, \tag{9}$$

where $\widehat{\text{CAPE}}$ denotes a computation performed assuming pseudoadiabatic ascent. The thermodynamic cycle considered in integrating the pseudoadiabatic equations does not assume that total water mixing ratio is conserved in the ascent, outflow, and descent legs. We note that the value of the irreversible entropy production is the same for reversible and pseudoadiabatic thermodynamics.

c. *Equivalence of PI forms*

1) Analytic formulas

Having related the mechanical work to the CAPE difference definition of PI and evaluated the work integrals, it is now straight-forward to connect the PI forms. Based on the different definitions of PI and the relations for reversible thermodynamics obtained in section 3b, we can see that

$$\text{PI}_C^2 = \text{PI}_k^2 + \frac{C_k}{C_D}\frac{T_s}{T_o}\left[c_l T_o \ln\left(\frac{T_o}{T_s}\right)\left(r_s^* - r_b\right) - T_o \Delta s_{\text{irr}}\right], \text{and} \tag{10}$$

$$\begin{aligned}\text{PI}_C^2 = \text{PI}_s^2 + \frac{C_k}{C_D}\frac{T_s}{T_o}\Big\{c_l\big[T_s(1 - \ln\ T_s) - T_o(1 - \ln\ T_o)\big] \\ \left(r_s^* - r_b\right) - T_s \Delta s_{\text{irr}}\Big\},\end{aligned} \tag{11}$$

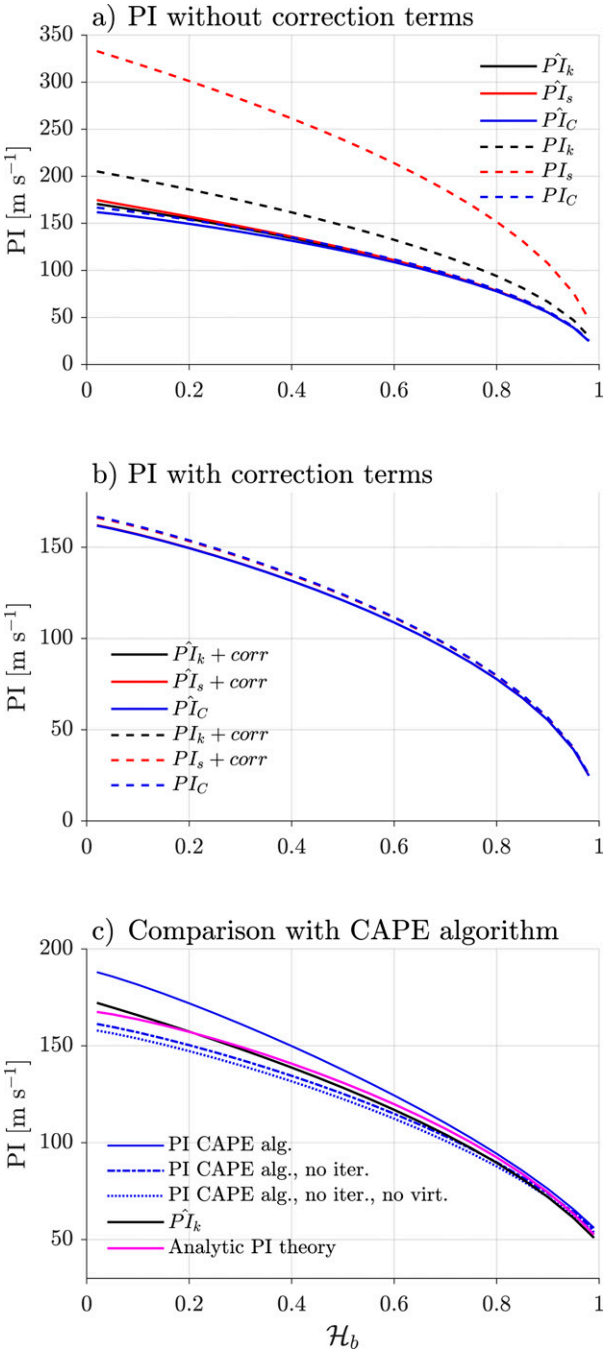

FIG. 2. (a) PI vs relative humidity for enthalpy Carnot PI [PI_k; black, (1)], entropy Carnot PI [PI_s; red, (2)] and CAPE PI [PI_C; blue, (3)] as a function of relative humidity, for both reversible (dashed lines) and pseudoadiabatic (solid lines) thermodynamics. (b) PI vs relative humidity for corrected enthalpy Carnot PI [PI_k; black, (10), (12)], corrected entropy Carnot PI [PI_s; red, (11), (13)] and CAPE PI [PI_C; blue, (3)] as a function of relative humidity, for both reversible (dashed lines) and pseudoadiabatic (solid lines) thermodynamics. The correction terms include the effects of both heat capacity and irreversible entropy production for the moist reversible thermodynamics formulation, and the effects of irreversible entropy production only for pseudoadiabatic thermodynamics.

so long as the effects of water vapor on density are neglected in the CAPE computations. We call the terms on the RHS that bring the entropy or enthalpy Carnot PI formulas to the CAPE expression "correction" terms.

Similarly, but more simply, for pseudoadiabatic thermodynamics, we have

$$\widehat{\mathrm{PI}}_C^2 = \widehat{\mathrm{PI}}_k^2 - \frac{C_k}{C_D} T_s \Delta s_{\mathrm{irr}}, \quad \text{and} \tag{12}$$

$$\widehat{\mathrm{PI}}_C^2 = \widehat{\mathrm{PI}}_s^2 - \frac{C_k}{C_D} \frac{T_s^2}{T_o} \Delta s_{\mathrm{irr}}. \tag{13}$$

2) NUMERICAL RESULTS

To test the analytic results of the previous section, we numerically evaluate the forms of PI and then add the correction terms to show that they do indeed lead to equivalence. The appearance of the irreversible entropy production term Δs_{irr} in all of the corrections suggests that a fruitful path to evaluate the analytic results is to consider a wide range of surface air relative humidity, as this term grows with subsaturation. Here, we perform calculations with no air–sea temperature difference, to clarify the differences between the entropy and enthalpy Carnot PI formulas in the simplest thermodynamic cycle that is consistent with the PI assumptions.

Figure 2a shows the comparison between the uncorrected PI formulations. If we take CAPE PI as a reference due to the close relation between the CAPE difference and the mechanical work produced by the cycle, we can see that a blunt application of the Carnot PI formulas, either based on reversible entropy or enthalpy leads to outlandishly high values of PI due to the effects of the changes in heat capacity on entropy or enthalpy. Conversely, pseudoadiabatic PI formulations only depart due to the irreversible entropy production term, which is small for Earthlike conditions. For $\mathcal{H}_b = 0.8$, we have $\sqrt{T_s \Delta s_{\mathrm{irr}}} \approx 8\,\mathrm{m\,s^{-1}}$. Because of the quadratic form of PI, this only leads to a 0.5% difference in PI. For much drier conditions such as $\mathcal{H}_b = 0.1$, the irreversible entropy production term leads to a 4% decrease in PI despite the much larger value of PI itself. This suggests that, to compute PI based on thermodynamic disequilibrium requires either neglecting changes to heat capacity in entropy and enthalpy, as in the pseudoadiabatic approximation, or adding an extra term accounting explicitly for those changes if using reversible thermodynamics. Doing otherwise would lead to an overestimation of the mechanical work that the cycle can produce and of PI. Since TCs are heavily precipitating, we suggest simply

←

(c) PI vs relative humidity with a 1-K air–sea temperature contrast, for the algorithm of Bister and Emanuel (2002) (solid blue), the algorithm without iterating on surface pressure (dash–dotted blue), the algorithm without iterating on surface pressure and neglecting virtual effects (dotted blue), the pseudoadiabatic enthalpy Carnot formula [solid black, (1)], and the newly introduced analytic formula based on an entraining plume CAPE formulation [solid magenta, (17)].

using pseudoadiabatic thermodynamics and neglecting the irreversible entropy terms for Earthlike applications.

Figure 2b verifies this reasoning by comparing all three forms of PI, with the added correction terms, for both reversible and pseudoadiabatic thermodynamics. The three forms of PI collapse onto two distinct profiles: one for reversible thermodynamics and one for pseudoadiabatic thermodynamics. Those two profiles do not depart much from one another due to the neglect of the effects of water species on density in the CAPE computation. The relative difference between corrected PI_k and PI_s is about 10^{-12}, while the relative difference between PI_C and corrected PI_k is about 0.002. This second value is larger, and may arise from inaccuracies in the numerical computation of CAPE, but it is still fairly small. For reference, merely choosing between different commonly used empirical relations to compute $e^*(T)$ causes similar fractional changes in PI_C (not shown).

d. List of equivalence conditions

To establish the requirements for the equivalence between PI forms, we started by integrating both reversible and pseudoadiabatic differential forms of thermodynamic equations around the PI cycle to obtain (6)–(9). From there, we obtained correction terms that establish precisely why the computations of PI from different forms depart from one another. In the pseudoadiabatic case, the only correction needed is to account for irreversible entropy production, which is negligible in Earthlike conditions, but not at low surface relative humidity. In the reversible case, an additional and much more important correction term arises from accounting for the variations of heat capacity. Our equations are valid if the following conditions are met:

1) the surface air–sea temperature difference is small,
2) pressure is constant along the inflow leg of the PI cycle,
3) we neglect the effects of water vapor on density, and
4) the outflow leg of the PI cycle matches an isothermal environment.

For Earthlike conditions, relaxing condition 1 does not have a large influence on the comparison of PI forms. Condition 2 is only an assumption with respect to certain PI theories (e.g., Emanuel 1988b), but is consistent with other forms (e.g., Bister and Emanuel 1998). Condition 3 has a nonnegligible effect, which we will quantify in section 5, and the validity of condition 4 depends on the upper-tropospheric stratification. In contrast to most literature on PI, we did not assume phase equilibrium in our derivations, which leads to the appearance of the irreversible entropy production correction term.

4. An approximate Carnot PI formula from CAPE definition

By integration over thermodynamic cycles, the previous section enumerated the conditions under which Carnot and CAPE PI are equal. But the physical connection between CAPE differences and the Carnot formulas remains enigmatic. This section utilizes the theory of Romps (2016) to shed light on this, first in a back-of-the-envelope fashion (section 4a) and then in greater detail (section 4b).

a. A napkin derivation

As discussed above, differences in CAPE are given by differences in work done during tropospheric ascent, which can also be written as vertical integrals of buoyancy differences Δb:

$$\Delta\mathrm{CAPE} = \int \Delta\alpha \, dp = \int \Delta b \, dz = \int \frac{\Delta b}{\Gamma} dT, \tag{14}$$

where $\Gamma = -dT/dz$ and we write the last integral in temperature coordinates, for reasons that will be clear in a moment. Now, Singh and O'Gorman (2013) showed that temperature differences ΔT between parcels at a given height can be expressed in terms of their moist static energy (MSE) differences Δh as $\Delta T = \Delta h/\beta$, where we use the Seeley and Romps (2015) version of this expression with $\beta = c_p + L dq_v^*/dT$ measuring how much of Δh will be expressed as sensible versus latent enthalpy. In the mid- and upper troposphere, latent enthalpies are small and $\beta \approx c_p$, so MSE differences will be expressed there as relatively large temperature (i.e., buoyancy) differences, yielding the well-known ballooning of buoyancy in the upper troposphere (the "shape of CAPE"; Seeley and Romps 2015). Romps (2016) further showed that for moist adiabats under Earthlike conditions, $\Gamma \approx g/\beta$. We can thus write the integrand in the last term on the RHS of (14) as

$$\Delta b \frac{1}{\Gamma} \approx g \frac{\Delta T}{T} \frac{\beta}{g} = \frac{\Delta h}{T} \, . \tag{15}$$

Thus, in temperature coordinates the buoyancy integrand is straightforwardly related to Δh, as the β factors cancel.

With this MSE–buoyancy relationship in hand, and specializing to the case of differences between the saturated "hurricane" parcel and the environmental parcel, and also invoking the definition (3) of CAPE PI, we have

$$\mathrm{PI}_C^2 = \frac{T_s}{T_o}\Delta\mathrm{CAPE} \approx \frac{T_s}{T_o}\int_{T_s}^{T_o} \frac{\Delta b}{\Gamma} dT \approx \frac{T_s}{T_o}(h^* - h_a)\frac{T_s - T_o}{T_{\mathrm{avg}}},$$

with tropospheric average temperature T_{avg} the mean of T_s and T_o. One thus recovers a Carnot-type expression from the CAPE definition, because the buoyancy difference is closely related to the MSE difference via (15), and (critically) because the MSE difference between these *particular* parcels is nearly identical to the air-surface disequilibrium in the Carnot formula (1). Note that the factor $(T_s - T_o)$ arises naturally in the vertical integration as the temperature depth of the troposphere.

This straightforward physical picture connecting the CAPE formula and the Carnot expression has not previously been described. In what follows, we present a complete version of this result (derived in appendix B), show an intuitive graphical representation of where the buoyancy contrast between the two parcels' profiles arises, describe the magnitude of the terms in the more complete expression, and evaluate the approximations.

b. Complete approximate PI formula from CAPE definition

Here, we review the CAPE theory of Romps (2016), apply it to derive an approximate PI formula, and evaluate the magnitude of its terms to reconcile it with (1).

1) REVIEW OF Romps (2016) CAPE THEORY

Romps (2016, hereafter R16) developed an analytical theory for CAPE by first deriving analytical formulas for moist adiabatic temperature and humidity profiles, allowing for the effects of dilution by entrainment. He then invoked the "zero buoyancy" plume model of Singh and O'Gorman (2013), which says that a tropical-mean temperature profile can be obtained as the temperature profile of a dilute moist adiabat (the corresponding entraining plume thus has zero buoyancy relative to the mean profile). This led R16 to a general analytic expression for tropical CAPE. Here, however, we are interested in a *difference* of CAPEs, which is independent of the environmental profile; we thus need not invoke the zero-buoyancy model, or make any other assumptions about the environmental profile. Instead, we simply apply R16's undilute, moist-adiabatic temperature and humidity profiles to the saturated "hurricane" and environmental parcels to calculate their CAPE difference.

A key to the R16 formalism is a change of coordinates from integrating the buoyancy ($\propto \Delta T$, neglecting virtual temperature effects) in altitude to integrating the buoyancy ($\propto \Delta z$) in temperature. With the change of coordinates ($\int \Delta T dz \rightarrow \int \Delta z dT$), CAPE is defined as

$$\mathrm{CAPE} = \frac{g}{T_{\mathrm{avg}}} \int_{T_o}^{T_s} [z_0(T) - z_{\mathrm{env}}(T)] dT, \tag{16}$$

with $z_0(T)$ being the height profile for a nondilute moist adiabat and $z_{\mathrm{env}}(T)$ being the height profile of the environment. The buoyancy is computed relative to the tropospheric average temperature $T_{\mathrm{avg}} = (T_s + T_0)/2$, an approximation of the theory. The T_o in (16) is the tropopause temperature that is assumed to be the same in the isothermal stratosphere above. R16 wrote this as T_{FAT} following the fixed-anvil temperature (FAT) hypothesis (Hartmann and Larson 2002), but T_o is used here for consistency with PI literature's outflow temperature.

Then, R16 expressed $z(T)$ in terms of special functions. These heights are given by the following formula, assuming the surface height is zero:

$$z(T) = z_{\mathrm{dry}}(T) + z_q(T),$$

where the first right-hand-side term corresponds to the height of a dry atmosphere $z_{\mathrm{dry}}(T) = c_p[T(z=0) - T]/g$ and the second term is the height that arises from humidity. This term is proportional to the amount of latent heat that has been released from the LCL to an isotherm T, asymptoting to a height $\propto L q^*_{\mathrm{LCL}}/g$ at cold temperatures when all of the latent heat has been released. Here, q denotes specific humidity, and the full expression for z_q can be found in appendix B.

2) EVALUATION OF PI WITH CAPE THEORY

The detailed derivation is presented in appendix B. The essence is that we evaluate the CAPE definition of PI (3) using the R16 profiles for our undilute parcels. The common environmental soundings cancel, leaving only the integrated buoyancy differences of the undilute parcels.

To gain an intuition for that analysis, we plot these heights in Fig. 3a (black lines) for representative conditions: $T_s = 300$ K, $T_a = 299$ K, $\mathcal{H}_b = 0.8$, and $T_o = 200$ K. The dashed line shows the height of the nonentraining parcel lifted from the environmental surface $\mathcal{H}_b$ and air temperature z_0^m and the solid line shows that of the saturated "hurricane" parcel z_0^*. The differences between these—with solid above dashed, implying positive buoyancy—are nearly vertically uniform in the temperature coordinate above the subcloud layer ($T \lesssim 295$ K). The moist component of height (B1) increases from the surface for the saturated parcel to the environmental LCL (blue solid line in Fig. 3), where the other parcel's moist component of height first becomes nonzero. This implies there is a nonzero subcloud contribution to PI, though the buoyancy above the LCL dominates for Earthlike conditions.

The result of the derivation is this new approximate PI expression:

$$\mathrm{PI}_C^2 = \frac{T_s}{T_o}\frac{c_k}{c_d}\frac{1}{T_{\mathrm{avg}}}\left\{c_p(T_s - T_a)(T_s - T_o) + L q_s^*(T_s - T_o) - L q_a (T^m_{\mathrm{LCL}} - T_o) - \frac{L}{\gamma}\left[q_s^* - q_a + \frac{L}{2RT_{\mathrm{avg}}}\left(q_s^{*2} - q_a^2\right)\right]\right\} \tag{17}$$

with fractional lapse rate of saturation specific humidity $\gamma = -\partial_z \log(q^*)$ (evaluated at T_{avg}). While the first three terms are close to the standard Carnot expression, the last two terms are distinct and arise from the subcloud buoyancy. The magnitude of these terms is described next. This new approximate PI formula is a central contribution of this research: we have used the R16 formulas for moist-adiabatic thermodynamic profiles, along with the CAPE-based definition of PI, to analytically derive a new approximate PI formula. The resulting expression involves familiar environmental quantities (e.g., T_s, T_a, T_o), as well as thermodynamic quantities embedded in the constant γ and the LCL temperature T_{LCL}.

3) MAGNITUDE OF TERMS

To reconcile this new analytic formula with (1), we examine the magnitude of the terms in the expression (17) for Earthlike conditions.

First, the subcloud humidity contributions are small compared to those of the free-troposphere (B4). This can be quantified by considering the magnitude of an upper bound on the subcloud term. Replacing the temperature-dependent saturation specific humidity $q^*(T)$ with that of the LCL, q^*_{LCL}, in the subcloud term provides the bound: $\int_{T_{\mathrm{LCL}}}^{T_s} (L/g)[q_s^* - q^*(T)] \le \int_{T_{\mathrm{LCL}}}^{T_s} (L/g)\left(q_s^* - q^*_{\mathrm{LCL}}\right) = (L/g)\left(q_s^* - q^*_{\mathrm{LCL}}\right)(T_s - T_{\mathrm{LCL}})$. Both the subcloud and free-troposphere terms now have a common $L\left(q^* - q^*_{\mathrm{LCL}}\right)/g$ that is multiplied by a temperature difference. The ratio of the subcloud to the free-troposphere temperature difference is ($T_{\mathrm{LCL}} - T_o = 100$ K to $T_s - T_{\mathrm{LCL}} = 5$ K) about 20. Alternatively, assuming the surface air humidity can be approximated by neglecting the air–sea temperature difference

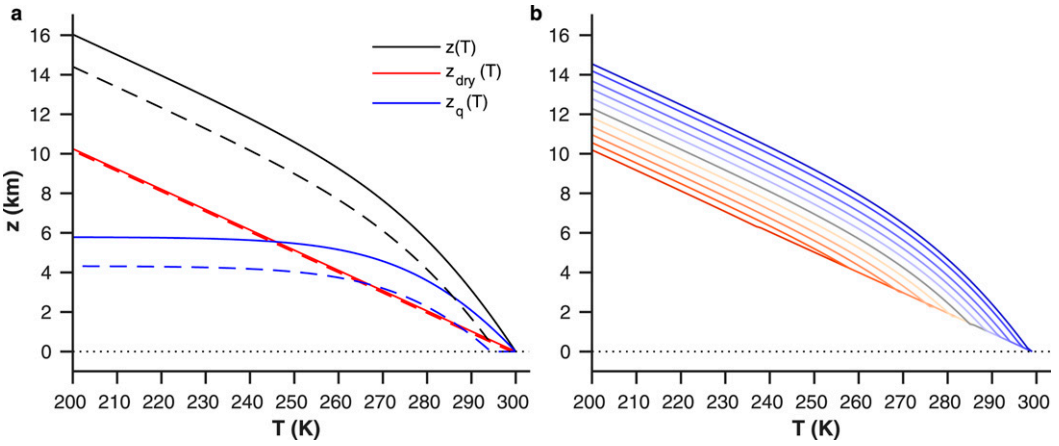

FIG. 3. (a) Height and its components [dry in red and humidity in blue; (B1)] vs temperature for the two nonentraining parcels that determine the PI (B3) for representative values of relative humidity, surface, surface air, and outflow temperatures. Potential intensity is proportional to the integral of the difference between the black solid and dashed curves. (b) Temperature vs height over a range of surface relative humidities with $\mathcal{H}_b = 0.5$ in gray, lower $\mathcal{H}_b$ in successively darker reds, and higher $\mathcal{H}_b$ in successively darker blues. The temperature soundings are shown for the nine integer multiples of $\mathcal{H}_b = N \times 0.1$ and $\mathcal{H}_b = 0.02, 0.98$.

$q_a \approx \mathcal{H}_b q_s^*$ and evaluating a Taylor expansion of q_s^* yields a similar result.

For the Earthlike regime with a negligible subcloud contribution, the new PI expression is

$$\mathrm{PI}_C^2 \approx \frac{T_s}{T_o}\frac{c_k}{c_d}\frac{1}{T_{\mathrm{avg}}}\Big[c_p(T_s - T_a)(T_s - T_o) + Lq_s^*(T_{\mathrm{LCL}}^m - T_o) - Lq_a(T_{\mathrm{LCL}}^m - T_o)\Big].$$

If the T_{LCL}^m is close to T_s, it becomes

$$\mathrm{PI}_C^2 = \frac{c_k}{c_d}\frac{T_s - T_o}{T_o}\left(k_s^* - k_a\right)\frac{T_s}{T_{\mathrm{avg}}}. \tag{18}$$

This series of approximations yields a form of the new PI expression that is nearly identical to (1). The additional factor of T_s/T_{avg} is ≈1.2 for Earthlike tropical values. This factor increases the climatological estimate of PI by 10% and would not substantially affect PI's temperature sensitivity.

The appearance of T_{avg}^{-1} in the CAPE-based PI formula that we present here arises from the R16 theory approximation of computing buoyancy relative to the tropospheric average temperature. If the buoyancy is instead computed relative to a density of surface temperature air [i.e., $T_{\mathrm{avg}} \to T_s$ in (16)], the above (18) would be identical to the PI Carnot formula (1). However, Seeley and Romps (2015) showed that undilute parcel buoyancy is large in the upper troposphere because the additional moist static energy of the undilute parcel is manifest as temperature—and therefore buoyancy—where the temperature is sufficiently cold. As a result, we do not think there is a well justified physical basis to alter the definition of CAPE used at the outset of our derivation to force the resulting PI expression to better conform to previous formulas.

5. Comparison to CAPE-based PI algorithm

This section evaluates the impacts of the equivalence conditions enumerated in section 3 on the CAPE-based PI algorithm, and also compares these results to the new approximate PI expression (17). Although CAPE PI should be largely independent of the environmental temperature profile, the CAPE–PI algorithm requires one as an input. For simplicity we use dilute moist adiabats obtained from the R16 formalism, consistent with the zero-buoyancy plume model. This is akin to using moist adiabats as approximate tropical temperature profiles, but including entrainment.

First, we use a representative Earthlike tropical sounding (R16 dilute adiabat plus representative surface RH) in the PI algorithm to assess the quantitative importance of factors neglected in both the derivation of the correction terms in section 3 and the new analytic formula in section 4. In particular, both assume constant surface pressure and omit virtual effects. Second, we consider a range of soundings with varying surface relative humidity. Not only was this a useful demonstration of the role of irreversible entropy production in the correction terms described in section 3, but it is also a climate variation that possibly distinguishes the new approximate PI formula (17) (with its dependence on both LCL and surface temperature) from the Carnot approximation (dependent on surface temperature).

The R16 dilute adiabats are specified by the surface air temperature T_a, the outflow temperature T_o, the surface relative humidity $\mathcal{H}_b$, and the nondimensional parameter characterizing the effect of entrainment on the temperature stratification a. We chose T_s = 300 K, T_a = 299 K, T_o = 200 K, $\mathcal{H}_b = 0.8$, and a = 0.2. This value of a is chosen to emulate the results of cloud-system-resolving model simulations of radiative convective equilibrium (R16), but results do not

TABLE 1. Results of the numerical CAPE-based PI algorithm (3) for the velocity PI (m s^{-1}) for an Earthlike sounding with T_s = 300 K (see section 5 for other sounding details) in the top row and the percentage increase in velocity PI in response to 1 K surface warming in the bottom row. The columns are variants of the algorithm to assess the magnitude of the approximations used in the derivation of (17), with the full description of the altered algorithms in section 5a.

Standard	No iteration	No virtual effect	Buoyancy approximation	All
94.3	89.9	91.4	94.2	87.8
4.1%	3.4%	3.8%	4.0%	3.3%

depend on this choice. We use the CAPE-based PI algorithm with the pseudoadiabatic ascent option, equal drag coefficients for momentum and enthalpy ($c_d = c_k$), dissipative heating included, and the algorithm's empirical wind reduction factor set to one (in contrast to the default value of 0.8). We use the MATLAB implementation of the PI algorithm, which is equivalent to the 2013 version of the Fortran code. The Carnot formula relies on the assumption of an isothermal outflow layer, so we add an isothermal stratosphere on top of the R16 soundings.

a. *Assessment of derivations' approximations*

We compare the results of the standard CAPE-based PI algorithm with altered algorithms that bring the numerical algorithm toward the R16 theory by using the same approximations. For the Earthlike sounding, the CAPE-based PI algorithm has a velocity PI of 94.3 m s^{-1} (Table 1, standard).

In the derivation of the equivalence conditions in section 3, the surface pressure was assumed constant, and in the numerical evaluations of thermodynamic quantities shown in Figs. 2a and 2b, it was chosen to be 10^5 Pa. Likewise, in the derivation of the new approximate form of PI from the R16 CAPE theory, we did not consider the effect of the TC pressure on CAPE. To assess the neglect of the TC pressure drop relative to the environment, we alter the CAPE-based PI algorithm by not iterating the parcel pressures to that of the pressure PI. In the numerical algorithm, we perform a single iteration, so that the parcel pressures of the CAPE calculations remain equal to that of the environment. Comparison of the values in Table 1 shows that this decreases the PI by ≈4.7% (no iteration).

We note that this is a much smaller effect of TC pressure on PI than that reported in some of the literature, starting with Emanuel (1988a). This occurs because the model of Emanuel (1988a) implies that the central pressure of the TC only influences the saturation parcel mixing ratio, while the model of Bister and Emanuel (2002) considers that the TC central pressure influences both the saturation and the environmental parcels, leading to a large cancellation of the pressure change effect in Bister and Emanuel (2002) and in the associated PI algorithm, but not in the model of Emanuel (1988a).

One of the assumptions in section 3 and in the R16 theory for CAPE is to neglect the virtual (water vapor) effect on density. To assess the omission of the virtual effect, we alter the buoyancy calculation, replacing virtual temperature with temperature, in the algorithm's CAPE subroutine. Table 1 shows that this decreases the PI by ≈3% (no virtual effect).

The R16 theory also assumes that the parcel (subscript p) buoyancy can be approximated by the ratio of the temperature difference relative to the environment (subscript e) and the tropospheric average temperature: $b \propto (T_p - T_e)/T_{\text{avg}}$. The PI algorithm computes CAPE as an integral in pressure, rather than altitude. Therefore, we replace the pressure of the R16 sounding—obtained by hydrostatic integration of the vertically varying temperature—with an approximate pressure that is a hydrostatic integration using the tropospheric average temperature T_{avg}. Table 1 shows that this increases the PI by ≈0.1% (buoyancy approximation). When all three approximations are used simultaneously, the PI decreases by ≈6.9% (Table 1, all), suggesting that these small approximations add close to linearly.

Table 1 also shows the percentage change in PI when the surface temperature is warmed by 1 K, holding the surface-to-air temperature difference fixed. One might take this to be a starting point for the magnitude of the sensitivity of PI to global warming; however, energetically consistent climate change simulations typically have decreases in the surface-to-air temperature difference and increases in surface relative humidity (e.g., Richter and Xie 2008), which would reduce the PI increase. The standard algorithm has a 4.1% increase in PI for this simple warming case and all of the algorithms have comparable sensitivities (Table 1, bottom row). For this perturbation, the new formula (17) has a 3.5% increase and the Carnot formula (1) has a 3.2% increase. This shows that the assumptions used in the derivation are modest not only in terms of the climatological PI, but also for the response to climate perturbations.

In summary, the conditions used to derive the equivalence of PI forms and the approximations used in the derivation of (17) modestly alter the PI for Earthlike conditions, when they are used in the numerical CAPE-based PI algorithm. This shows that climatological values of PI can be recovered with the simplifications used in the derivations. Furthermore, the sensitivity to a simple warming case is little changed by these approximations.

b. *Application to surface relative humidity changes*

The Carnot approximate PI formula (1) and the newly derived CAPE-based approximate PI formula (17) have similar dependence on outflow temperature T_o and sea surface temperature T_s. Therefore, we turn again to changes in surface relative humidity $\mathcal{H}_b$.

The CAPE-based approximate formula (17) will have increasing PI from increasing surface–air disequilibrium, like the Carnot formula, but it also has a dependence on $\mathcal{H}_b$ through the LCL saturation specific humidity q^*_{LCL}. Figure 3b shows temperature versus height for a series of surface relative humidity varying from 0.02 to 0.98 (all other parameters

constant with the parameter values described above). The lowest relative humidity (darkest red) produces a sounding similar to a dry adiabat, while the highest relative humidity (darkest blue) has a lapse rate that is affected by latent heat release essentially from the surface. The LCL rises in altitude and decreases in temperature as the surface relative humidity decreases (Fig. 3b). This, according to the new approximate PI formula, would decrease the PI relative to the Carnot formula.

The CAPE-based PI algorithm varies from velocity PI near 190 to 55 m s^{-1} across this range of soundings (Fig. 2c, blue solid line). Taking the Earthlike $\mathcal{H}_b = 0.8$ to be the reference case, the Carnot PI is 6% smaller than the algorithm, and the new formula is only 2% smaller. The algorithm's iteration on surface pressure increases the PI sensitivity (Fig. 2c, blue solid line vs blue dashed–dotted line) to $\mathcal{H}_b$ while there are minimal changes from eliminating virtual effects in the algorithm (Fig. 2c, blue dashed–dotted line vs blue dotted line). The Carnot formula has a weaker sensitivity to $\mathcal{H}_b$ than the original algorithm (Fig. 2c, black line vs blue line), but a higher sensitivity than the version of the algorithm that removes both virtual effects and iterations (Fig. 2c, black line vs dotted blue line) and this is consistent with the difference between $\widehat{\mathrm{PI}}_k$ and $\widehat{\mathrm{PI}}_C$ when neglecting irreversible entropy production. Figure 2c also shows that the new approximate formula (magenta line) yields very similar PI values to the Carnot formula (black line) for all values of $\mathcal{H}_b$, albeit with a slightly higher sensitivity at low $\mathcal{H}_b$ and a lower sensitivity at high $\mathcal{H}_b$. This difference is likely due to changes in LCL temperature, and the overall differences are modest for the Earthlike regime of relative humidity $\gtrsim 0.7$.

We note that since we effectively enforce different near–surface thermodynamic disequilibrium for all $\mathcal{H}_b$, the sensitivities of PI to drying presented here are not directly comparable to those of studies that instead enforce surface energy balance (e.g., Cronin and Chavas 2019).

In summary, both the Carnot formula and new approximate formula slightly overestimate the sensitivity to systematically varied surface-air relative humidity compared to a numerical CAPE-based calculation with the same assumptions and underestimate the sensitivity compared to the CAPE–PI algorithm. Nevertheless, these differences only emerge for fairly low surface relative humidity, rather than in Earthlike situations.

6. Conclusions

Potential intensity (PI) theory plays an important role in climate change discourse about tropical cyclones (e.g., Sobel et al. 2016). For example, there is confidence in the expectation that the intensity of the most intense tropical cyclones will increase as a result of warming because it is found in both simulations (e.g., Knutson and Tuleya 2004) and PI theory (Emanuel 1987). The tropical-mean PI increase is robustly simulated and has previously been interpreted in terms of the Carnot-cycle based approximate PI formula that depends on the air–sea enthalpy disequilibrium, which increases with warming. However, quantitative assessments of PI changes in climate models use the iterative numerical CAPE-based algorithm, where it is less clear why PI increases with warming.

Here, we presented a new analysis of when the Carnot and CAPE PI definitions are equivalent. The CAPE PI definition is equal to the mechanical work produced by the TC cycle, under conditions we enumerated. Independent of the thermodynamic formulas, there is an irreversible entropy production term in the TC cycle that has previously been ignored, and this term must be added to the Carnot definition of PI to make it equivalent to the CAPE definition. For reversible thermodynamics, an additional correction term that accounts for heat capacity changes is needed to reduce the Carnot PI to the CAPE PI. Our numerical assessment of the analytic formulas that connect the PI forms successfully captures the PI dependence on surface relative humidities, where factor of ≈4 variation in PI provides a stringent test.

We also used the CAPE-based definition of PI to provide a physical interpretation for the Carnot form by building on recent advances in the understanding of CAPE. The essence is that the buoyancy difference between the two parcels that determine the PI's CAPE difference result from surface moist static energy contrasts, which become buoyancy contrasts as latent heat is released over the temperature depth of the troposphere. This can be formalized using the CAPE theory of R16 in the CAPE definition of PI. The resulting approximate PI formula and its sensitivity to warming are comparable to the previously discussed approximate Carnot form of PI, though the new formula's PI is ≈10% higher. The derivation uses approximations that lead to modest ≈5% changes when the CAPE-based algorithm is modified to use the same approximations (Table 1), suggesting no quantitatively important errors are introduced in our derivation of an approximate PI formula.

The research presented here connects the numerical CAPE PI algorithm, based on the CAPE definition of PI, to the more physically intuitive Carnot definitions, and provides a new approximate formula derived from the CAPE definition that is quite similar to the existing Carnot approximate formula. This bridges the gap between the quantitative technique used to assess future climate model projections and the physical explanation for the increase in PI under warming as the result of near-surface thermodynamic changes.

Acknowledgments. The authors thank Kerry Emanuel for providing the PI-CAPE code (ftp://texmex.mit.edu/pub/emanuel/TCMAX/). Two anonymous reviewers and Dan Chavas provided helpful feedback. We thank Stephen Garner, Paul O'Gorman, Adam Sobel, and Wenyu Zhou for motivating discussions, and Stephen Garner and Hiroyuki Murakami for comments on a draft of the manuscript. TM was supported by a NSERC Discovery grant and Canada Research Chair (Tier 2).

Data availability statement. The code to reproduce the figures is available at https://web.meteo.mcgill.ca/~tmerlis/code/rousseau-rizzi_etal21_cape_pi_code_rev1.tgz.

APPENDIX A

Irreversible Entropy Production Integral

The integral of the irreversible entropy production vanishes on the ascent, outflow and descent legs, because, over these legs, the air is either saturated, or has constant r. This allows us to write the integral over the isothermal and constant pressure inflow leg as

$$\oint -TR_v \ln(\mathcal{H})dr = -T_s R_v \int_{r_b}^{r_s^*} \ln(\mathcal{H})dr. \tag{A1}$$

Using the definition $\mathcal{H} = e/e^*$, and the fact that $e^*(T)$ is constant over the inflow leg, we may write

$$\int_{r_b}^{r_s^*} \ln(\mathcal{H})dr = \int_{r_b}^{r_s^*} \ln(e) - \ln(e^*)dr = -\ln\left(e_s^*\right)\left(r_s^* - r_b\right) + \int_{r_b}^{r_s^*} \ln(e)dr. \tag{A2}$$

Then, integrating by part, and making use of the definition of r, and of the fact that pressure is constant we obtain

$$\int_{r_b}^{r_s^*} \ln(\mathcal{H})dr = -\ln\left(e_s^*\right)\left(r_s^* - r_b\right) + r_s^* \ln\left(e_s^*\right) - r_b \ln(e_b) + \varepsilon \int_{e_b}^{e_s^*} d\ln(p-e). \tag{A3}$$

Simplifying by collecting terms and making use of the definition of $\mathcal{H}$, we find

$$\oint -TR_v \ln(\mathcal{H})dr = T_s R_v \left[r_b \ln(\mathcal{H}_b) + \varepsilon \ln\left(\frac{p_s - e_b}{p_s - e_s^*}\right)\right]. \tag{A4}$$

This solution can be rearranged by making use of the definitions of $\mathcal{H}$, r, and ε, to eliminate the less intuitive e:

$$\oint -TR_v \ln(\mathcal{H})dr = T_s R_v \left[r_b \ln(\mathcal{H}_b) + \varepsilon \ln\left(\frac{r_s^* \mathcal{H}_b}{r_b}\right)\right], \tag{A5}$$

or

$$\Delta s_{\text{irr}} = R_v \left[r_b \ln(\mathcal{H}_b) + \varepsilon \ln\left(\frac{r_s^* \mathcal{H}_b}{r_b}\right)\right]. \tag{A6}$$

APPENDIX B

Derivation of an Approximate PI Formula Using R16

In this appendix, we will substitute the R16 theory for CAPE (16) into the CAPE PI formula (3) to derive a new approximate PI formula (17) that is similar to the Carnot expression.

First, the R16 formula for the height that arises from humidity is

$$z_q(T) = \frac{L}{g(1+a)}\left[q_{\text{LCL}}^* - q^*(T)\right] H(T - T_{\text{LCL}}), \tag{B1}$$

where H is the Heaviside step function and the nondimensional parameter a is defined as $a = \text{PE}\varepsilon/\gamma$, with precipitation efficiency PE (nondimensional, defined as the ratio of net condensation to gross condensation), fractional entrainment rate ϵ (dimensions of inverse length), and fractional lapse rate of saturation specific humidity $\gamma = -\partial_z \log(q^*)$ (dimensions of inverse length). The theory's saturation specific humidity above the parcel's LCL is

$$q^*(T) = (1+a)\frac{RT_{\text{avg}}}{L} W\left[y e^{-\gamma(T_{\text{LCL}} - T)}\right] \tag{B2}$$

where W (the Lambert W function), constant γ, and constant y are defined as

$$W(x\exp^x) = x,$$

$$\gamma = \frac{L}{R_v T_{\text{avg}}^2} - \frac{c_p}{RT_{\text{avg}}},$$

$$y = \frac{Lq_{\text{LCL}}^*}{(1+a)RT_{\text{avg}}} \exp\left[\frac{Lq_{\text{LCL}}^*}{(1+a)RT_{\text{avg}}}\right].$$

Note that a given parcel, particularly the hurricane parcel, can reach saturation at a level that is distinct from the environmental LCL. If $a = 0$, a moist pseudoadiabat is recovered. This constant, which affects the climatological dry stability and CAPE, does not affect the PI formula that we derive below.

There are differences in the formula that we presented above and R16. First, there are changes in some variables to avoid potential confusion in the context of TCs and PI. More importantly, the subcloud layer is ignored in R16, which eliminates the step function from (B1) and reduces the LCL quantities to surface quantities ($T_{\text{LCL}} \to T_s$ and $q_{\text{LCL}}^* \to q_s^*$). The inclusion of the subsaturated subcloud layer was not necessary in R16 because it is not important to the temperature dependence of CAPE discussed there. Here, it is retained because of the critical importance of the difference in the humidity of the parcel used to evaluate the two CAPEs in (3) and to recover the nonzero PI of a dry atmosphere with an air–sea surface temperature difference.

Here we substitute (16) into (3) and expand the difference between the hurricane CAPE and the environmental CAPE:

$$\text{PI}_C^2 = \frac{T_s}{T_o}\frac{c_k}{c_d}(\text{CAPE}^* - \text{CAPE}^m) = \frac{T_s}{T_o}\frac{c_k}{c_d}\frac{g}{T_{\text{avg}}}\left\{\int_{T_o}^{T_s}\left[z_0^*(T) - z_{\text{env}}(T)\right]dT - \int_{T_o}^{T_s}\left[z_0^m(T) - z_{\text{env}}(T)\right]dT\right\}.$$

Clearly, there is a common environmental height $z_{\text{env}}(T)$ that can be eliminated (see also, Garner 2015), and this also eliminates a sensitivity to entrainment rate:

$$\mathrm{PI}_C^2 = \frac{T_s}{T_o}\frac{c_k}{c_d}\frac{g}{T_{\mathrm{avg}}}\int_{T_o}^{T_s}\left[z_0^*(T) - z_0^m(T)\right]dT. \tag{B3}$$

Now, the integrand is the remaining height difference, $\Delta z = z_0^*(T) - z_0^m(T)$, of the two nonentraining ($a = 0$) parcels.

The dry component of the height integrates to $c_p(T_s - T_a)(T_s - T_o)/g$ in (B3), and the moist component can be handled as follows. The integral can be split into components above and below the LCL:

$$\int_{T_o}^{T_s}\Delta z_q dT = \int_{T_{\mathrm{LCL}}^m}^{T_s}\Delta z_q dT + \int_{T_o}^{T_{\mathrm{LCL}}^m}\Delta z_q dT.$$

Above the LCL, the temperature-dependent $q^*(T)$ terms in (B1) nearly exactly cancel, with modest deviations as y and the LCL do differ between the parcels [see (B2)]. This leaves a humidity difference constant in temperature $q_s^* - q_{\mathrm{LCL}}^*$:

$$\int_{T_o}^{T_{\mathrm{LCL}}^m}\Delta z_q dT = \frac{L}{g}\left(q_s^* - q_a\right)\left(T_{\mathrm{LCL}}^m - T_o\right), \tag{B4}$$

where we assume the humidity is constant from the surface air q_a to the LCL ($q_{\mathrm{LCL}}^* = q_a$). Next, the integrated subcloud buoyancy from humidity $L\Delta q/g$ can be obtained with the following change of variables:

$$\begin{aligned}
\int_{T_{\mathrm{LCL}}}^{T_s} q^*(T)dT &= (1+a)\frac{RT_{\mathrm{avg}}}{L}\int_{T_{\mathrm{LCL}}}^{T_s} W\left[ye^{-\gamma(T_s - T)}\right]dT, \quad \text{now let } u = ye^{-\gamma(T_s - T)},\ dT = \frac{1}{\gamma}\frac{du}{u}\\
&= (1+a)\frac{RT_{\mathrm{avg}}}{L\gamma}\int_{u_{\mathrm{LCL}}}^{u_s}\frac{W(u)}{u}du, \quad \text{now let } v = W(u),\ \frac{du}{u} = (1 + 1/v)dv\\
&= (1+a)\frac{RT_{\mathrm{avg}}}{L\gamma}\int_{v_{\mathrm{LCL}}}^{v_s}(1+v)dv\\
&= (1+a)\frac{RT_{\mathrm{avg}}}{L\gamma}\left(v + \frac{1}{2}v^2\right)\Big|_{v_{\mathrm{LCL}}}^{v_s}\\
&= (1+a)\frac{RT_{\mathrm{avg}}}{L\gamma}\left\{W(y) - W\left[ye^{-\gamma(T_s - T_{\mathrm{LCL}})}\right] + \frac{1}{2}W^2(y) - \frac{1}{2}W^2\left[ye^{-\gamma(T_s - T_{\mathrm{LCL}})}\right]\right\}\\
&= \frac{1}{\gamma}\left[q_s^* - q_{\mathrm{LCL}}^* + \frac{L}{2(1+a)RT_{\mathrm{avg}}}\left(q_s^{*2} - q_{\mathrm{LCL}}^{*2}\right)\right],
\end{aligned}$$

where the last step uses R16 theory for saturation specific humidity (B2). Note that q_{LCL}^* in the last line is really q^* at T_{LCL} along the surface parcel's moist adiabat, and that this adiabat will reach the temperature T_{LCL} at a slightly different pressure than the actual LCL. But for Earthlike relative humidity values this pressure difference is small, and we may approximate this as q_{LCL}^*. The full PI expression, after assuming $q_{\mathrm{LCL}}^* = q_a$, is then

$$\mathrm{PI}_C^2 = \frac{T_s}{T_o}\frac{c_k}{c_d}\frac{1}{T_{\mathrm{avg}}}\left\{c_p(T_s - T_a)(T_s - T_o) + Lq_s^*(T_s - T_o) - Lq_a \times \left(T_{\mathrm{LCL}}^m - T_o\right) - \frac{L}{\gamma}\left[q_s^* - q_a + \frac{L}{2RT_{\mathrm{avg}}}\left(q_s^{*2} - q_a^2\right)\right]\right\}. \tag{B5}$$

REFERENCES

Bister, M., and K. A. Emanuel, 1998: Dissipative heating and hurricane intensity. *Meteor. Atmos. Phys.*, **65**, 233–240, https://doi.org/10.1007/BF01030791.

——, and ——, 2002: Low frequency variability of tropical cyclone potential intensity 1. Interannual to interdecadal variability. *J. Geophys. Res.*, **107**, 4801, https://doi.org/10.1029/2001JD000776.

Bryan, G. H., 2008: On the computation of pseudoadiabatic entropy and equivalent potential temperature. *Mon. Wea. Rev.*, **136**, 5239–5245, https://doi.org/10.1175/2008MWR2593.1.

——, and R. Rotunno, 2009: Evaluation of an analytical model for the maximum intensity of tropical cyclones. *J. Atmos. Sci.*, **66**, 3042–3060, https://doi.org/10.1175/2009JAS3038.1.

Camargo, S. J., K. A. Emanuel, and A. H. Sobel, 2007: Use of a genesis potential index to diagnose ENSO effects on tropical cyclone genesis. *J. Climate*, **20**, 4819–4834, https://doi.org/10.1175/JCLI4282.1.

Chavas, D. R., K. A. Reed, and J. A. Knaff, 2017: Physical understanding of the tropical cyclone wind-pressure relationship. *Nat. Commun.*, **8**, 1360, https://doi.org/10.1038/s41467-017-01546-9.

Cronin, T. W., and D. R. Chavas, 2019: Dry and semidry tropical cyclones. *J. Atmos. Sci.*, **76**, 2193–2212, https://doi.org/10.1175/JAS-D-18-0357.1.

Emanuel, K. A., 1986: An air–sea interaction theory for tropical cyclones. Part I: Steady-state maintenance. *J. Atmos. Sci.*, **43**, 585–605, https://doi.org/10.1175/1520-0469(1986)043<0585:AASITF>2.0.CO;2.

——, 1987: The dependence of hurricane intensity on climate. *Nature*, **326**, 483–485, https://doi.org/10.1038/326483a0.

——, 1988a: The maximum intensity of hurricanes. *J. Atmos. Sci.*, **45**, 1143–1155, https://doi.org/10.1175/1520-0469(1988)045<1143:TMIOH>2.0.CO;2.

——, 1988b: Observational evidence of slantwise convective adjustment. *Mon. Wea. Rev.*, **116**, 1805–1816, https://doi.org/10.1175/1520-0493(1988)116<1805:OEOSCA>2.0.CO;2.

——, 1994: *Atmospheric Convection.* Oxford University Press, 580 pp.

——, 2003: Tropical cyclones. *Annu. Rev. Earth Planet. Sci.*, **31**, 75–104, https://doi.org/10.1146/annurev.earth.31.100901.141259.

——, 2013: Downscaling CMIP5 climate models shows increased tropical cyclone activity over the 21st century. *Proc. Natl. Acad. Sci. USA*, **110**, 12 219–12 224, https://doi.org/10.1073/pnas.1301293110.

——, C. DesAutels, C. Holloway, and R. Korty, 2004: Environmental control of tropical cyclone intensity. *J. Atmos. Sci.*, **61**, 843–858, https://doi.org/10.1175/1520-0469(2004)061<0843:ECOTCI>2.0.CO;2.

——, R. Sundararajan, and J. Williams, 2008: Hurricanes and global warming: Results from downscaling IPCC AR4 simulations. *Bull. Amer. Meteor. Soc.*, **89**, 347–368, https://doi.org/10.1175/BAMS-89-3-347.

——, S. Solomon, D. Folini, S. Davis, and C. Cagnazzo, 2013: Influence of tropical tropopause layer cooling on Atlantic hurricane activity. *J. Climate*, **26**, 2288–2301, https://doi.org/10.1175/JCLI-D-12-00242.1.

Garner, S., 2015: The relationship between hurricane potential intensity and CAPE. *J. Atmos. Sci.*, **72**, 141–163, https://doi.org/10.1175/JAS-D-14-0008.1.

Gilford, D. M., S. Solomon, and K. A. Emanuel, 2017: On the seasonal cycles of tropical cyclone potential intensity. *J. Climate*, **30**, 6085–6096, https://doi.org/10.1175/JCLI-D-16-0827.1.

Hartmann, D. L., and K. Larson, 2002: An important constraint on tropical cloud-climate feedback. *Geophys. Res. Lett.*, **29**, 1951, https://doi.org/10.1029/2002GL015835.

Knutson, T. R., and R. E. Tuleya, 2004: Impact of CO_2-induced warming on simulated hurricane intensity and precipitation: Sensitivity to the choice of climate model and convective parameterization. *J. Climate*, **17**, 3477–3495, https://doi.org/10.1175/1520-0442(2004)017<3477:IOCWOS>2.0.CO;2.

——, and Coauthors, 2010: Tropical cyclones and climate change. *Nat. Geosci.*, **3**, 157–163, https://doi.org/10.1038/ngeo779.

Merlis, T. M., and I. M. Held, 2019: Aquaplanet simulations of tropical cyclones. *Curr. Climate Change Rep.*, **5**, 185–195, https://doi.org/10.1007/s40641-019-00133-y.

——, W. Zhou, I. M. Held, and M. Zhao, 2016: Surface temperature dependence of tropical cyclone-permitting simulations in a spherical model with uniform thermal forcing. *Geophys. Res. Lett.*, **43**, 2859–2865, https://doi.org/10.1002/2016GL067730.

Nolan, D. S., E. D. Rappin, and K. A. Emanuel, 2007: Tropical cyclogenesis sensitivity to environmental parameters in radiative–convective equilibrium. *Quart. J. Roy. Meteor. Soc.*, **133**, 2085–2107, https://doi.org/10.1002/qj.170.

Persing, J., and M. T. Montgomery, 2003: Hurricane superintensity. *J. Atmos. Sci.*, **60**, 2349–2371, https://doi.org/10.1175/1520-0469(2003)060<2349:HS>2.0.CO;2.

Ramsay, H. A., M. S. Singh, and D. R. Chavas, 2020: Response of tropical cyclone formation and intensification rates to climate warming in idealized simulations. *J. Adv. Model. Earth Syst.*, **12**, e2020MS002086, https://doi.org/10.1029/2020MS002086.

Richter, I., and S.-P. Xie, 2008: Muted precipitation increase in global warming simulations: A surface evaporation perspective. *J. Geophys. Res.*, **113**, D24118, https://doi.org/10.1029/2008JD010561.

Romps, D. M., 2014: An analytical model for tropical relative humidity. *J. Climate*, **27**, 7432–7449, https://doi.org/10.1175/JCLI-D-14-00255.1.

——, 2016: Clausius–Clapeyron scaling of CAPE from analytical solutions to RCE. *J. Atmos. Sci.*, **73**, 3719–3737, https://doi.org/10.1175/JAS-D-15-0327.1.

Rousseau-Rizzi, R., and K. Emanuel, 2019: An evaluation of hurricane superintensity in axisymmetric numerical models. *J. Atmos. Sci.*, **76**, 1697–1708, https://doi.org/10.1175/JAS-D-18-0238.1.

——, and ——, 2021: A weak temperature gradient framework to quantify the causes of potential intensity variability in the tropics. *Climate*, **34**, 8669–8682, https://doi.org/10.1175/JCLI-D-21-0139.1.

——, R. Rotunno, and G. Bryan, 2021: A thermodynamic perspective on steady-state tropical cyclones. *J. Atmos. Sci.*, **78**, 583–593, https://doi.org/10.1175/JAS-D-20-0140.1.

Seeley, J. T., and D. M. Romps, 2015: Why does tropical convective available potential energy (CAPE) increase with warming? *Geophys. Res. Lett.*, **42**, 10 429–10 437, https://doi.org/10.1002/2015GL066199.

Singh, M. S., and P. A. O'Gorman, 2013: Influence of entrainment on the thermal stratification in simulations of radiative-convective equilibrium. *Geophys. Res. Lett.*, **40**, 4398–4403, https://doi.org/10.1002/grl.50796.

Smith, R. K., M. T. Montgomery, and S. Vogl, 2008: A critique of Emanuel's hurricane model and potential intensity theory. *Quart. J. Roy. Meteor. Soc.*, **134**, 551–561, https://doi.org/10.1002/qj.241.

Sobel, A. H., and S. J. Camargo, 2011: Projected future seasonal changes in tropical summer climate. *J. Climate*, **24**, 473–487, https://doi.org/10.1175/2010JCLI3748.1.

——, ——, T. M. Hall, C.-Y. Lee, M. K. Tippett, and A. A. Wing, 2016: Human influence on tropical cyclone intensity. *Science*, **353**, 242–246, https://doi.org/10.1126/science.aaf6574.

——, ——, and M. Previdi, 2019: Aerosol versus greenhouse gas effects on tropical cyclone potential intensity and the hydrologic cycle. *J. Climate*, **32**, 5511–5527, https://doi.org/10.1175/JCLI-D-18-0357.1.

Tang, B., and K. Emanuel, 2012: A ventilation index for tropical cyclones. *Bull. Amer. Meteor. Soc.*, **93**, 1901–1912, https://doi.org/10.1175/BAMS-D-11-00165.1.

Vecchi, G. A., and B. J. Soden, 2007: Increased tropical Atlantic wind shear in model projections of global warming. *Geophys. Res. Lett.*, **34**, L08702, https://doi.org/10.1029/2006GL028905.

——, S. Fueglistaler, I. M. Held, T. R. Knutson, and M. Zhao, 2013: Impacts of atmospheric temperature trends on tropical cyclone activity. *J. Climate*, **26**, 3877–3891, https://doi.org/10.1175/JCLI-D-12-00503.1.

Wang, S., S. J. Camargo, A. H. Sobel, and L. M. Polvani, 2014: Impact of the tropopause temperature on the intensity of tropical cyclones: An idealized study using a mesoscale model. *J. Atmos. Sci.*, **71**, 4333–4348, https://doi.org/10.1175/JAS-D-14-0029.1.

Wing, A. A., K. Emanuel, and S. Solomon, 2015: On the factors affecting trends and variability in tropical cyclone potential intensity. *Geophys. Res. Lett.*, **42**, 8669–8677, https://doi.org/10.1002/2015GL066145.

Zhou, W., I. M. Held, and S. T. Garner, 2014: Parameter study of tropical cyclones in rotating radiative–convective equilibrium with column physics and resolution of a 25-km GCM. *J. Atmos. Sci.*, **71**, 1058–1069, https://doi.org/10.1175/JAS-D-13-0190.1.